Contents lists available at ScienceDirect

Journal of Magnetism and Magnetic Materials

Frequency dependence of Néel temperature in CaMnO$_{3-\delta}$ ceramics: Synthesized by two different methods

A. Kompany, T. Ghorbani-Moghadam*, S. Kafash, M. Ebrahimizadeh Abrishami

Materials and Electroceramics Laboratory, Department of Physics, Ferdowsi Universityof Mashhad, Mashhad, Iran

A B S T R A C T

Calcium manganese oxide CaMnO$_{3-\delta}$ ($\delta = 0.02$) nanopowders were synthesized by two different methods; sol–gel and solid-state reaction. X-ray diffraction patterns indicated that both types of the prepared powders have orthorhombic symmetry structures at room temperature. Further characterizations of the samples were preformed employing SEM and TEM techniques. At low magnetic fields, the phase transition temperature from antiferromagnetic to paramagnetic was found to be slightly higher in the sintered O-ring shape specimens made from powders synthesized by sol–gel method. This result can be described in relation to Mn^{3+}–O–Mn^{4+} double-exchange interaction and also electron hopping mechanism which occur more in these specimens than those made from solid-state reaction powders. The frequency dependence of Néel temperature and the shape of the hysteresis loops, observed in both types of the prepared ceramics specimens, can be attributed to the reduction of relaxation time which occurs with increasing the frequency.

© 2013 Elsevier B.V. All rights reserved.

1. Introduction

Manganese oxides based compounds, because of their interesting thermoelectric, electrical, and magnetic properties have attracted many attentions in the past two decades [1–3]. These compounds have unusual charge and spin-orbital ordering showing large magnetoresistance property. However, temperature, pressure, applied field, doping and the method of preparation can alter some of their properties significantly [4–6]. Manganese oxide compounds based on CaMnO$_3$ have applications in fabricating many devices such as: cathode materials used in solid fuel cells, oxygen sensors and magnetoresistance switchings [2,7,8]. CaMnO$_3$ is a G-type antiferromagnetic (AFM) insulator with perovskite structure and Pnma space group. It has an additional weak ferromagnetic component in its ground state [9]. In the case of its cubic structure, the 5d orbitals of Mn ion split into three fold t$_{2g}$ and two fold e$_g$ orbitals. The t$_{2g}$ orbitals are perpendicular to the direction of 2p orbitals of oxygen and the electrons have a weak superexchang interaction with the neighboring Mn ions through 2p orbitals. When the oxygen content is decreased, the CaMnO$_{3-x}$($x=0-0.5$) phases show stronger double exchange interactions with ferromagnetic ordering. This can lead to the increase of Néel temperature, which has been reported by some workers [6,7,10,11]. In CaMnO$_{2.5}$, the antiferromagnetic transition to paramagnetic occurs at $T_N \sim 350$ K [12]. These effects are explained by the incorporation of Mn^{3+} cations, related to oxygen deficiency [6]. In Mn^{3+} ions, e$_g$ orbitals are aligned and

have overlapped with 2p orbitals of oxygen causing a strong superexchange interaction. In this case, degeneracy of e$_g$ orbitals has a significant effect on the ferro and antiferromagnetic properties of the sample, depending on which orbitals overlap. In CaMnO$_3$, the Mn^{3+}–O–Mn^{4+} interactions are induced by substituting the manganese sites with pentavalent or hexavalent cations or oxygen deficiency [11]. In the Mn^{3+}–O–Mn^{4+} interactions, the valence of Mn ions is changed by simultaneous electron hopping from e$_g$ orbitals of Mn^{3+} to p orbitals of oxygen and from oxygen orbitals to empty e$_g$ in Mn^{4+} ions. This phenomenon is known as double exchange interaction, which was first proposed by Zener [13–16].

Many works have been reported in relation to the structural and magnetic properties of CaMnO$_3$ at high magnetic fields [17–21], but up to our knowledge the relaxation behavior of the Néel temperature of CaMnO$_{3-\delta}$ ceramic has not been reported. In this work, we report the synthesis of CaMnO$_{3-\delta}$ in ceramic form made from nanopowders prepared by sol–gel and solid-state reaction techniques. Also, some magnetic properties including Néel temperature, hysteresis loops, and in particular, the frequency dependent behavior at low magnetic fields ($H < 30$ A/m) have been studied. In addition, the relaxation behavior of the Néel temperature has been investigated for both specimens.

2. Experimental

Powders of CaMnO$_{3-\delta}$ were synthesized via sol–gel and solid-state reaction methods, starting with a stoichiometric mixture of Ca (CH$_3$COO)$_2 \cdot X$H$_2$O and Mn(CH$_3$COO)$_2 \cdot 4$H$_2$O (99.9% purity, Merk).

* Corresponding author. Tel.: +989151041106.
E-mail address: ta_gh63@yahoo.com (T. Ghorbani-Moghadam).

In solid-state reaction, powders were prepared by mixing the starting materials with equal molar proportions. Then, the mixture was dried and ground to obtain a dark brown powder. In the sol–gel rout, the precursor materials were added gradually to distilled water kept at 40–45 °C. The clear sol was obtained without any precipitation by adding proper amounts of acetic acid and diethanolamine. The soft gel was formed by evaporating the solution after 16 h non-direct heating. Finally, a black powder was obtained by removing the organic compounds from the gel at 160 °C. All the synthesized powders were calcined at different temperatures, ranging from 700 to 900 °C for 2 h. Calcination of the powders was carried out by increasing the temperature at the rate of 2 °C/min up to the desired temperature, keeping the powders for 2 h at this temperature and then decreasing the temperature with at the same rate to room temperature. However, the lowest temperature at which manganese oxides perovskite structure formed was found to be 800 °C in earlier work [11]. X-ray diffraction (XRD: Advance- BrukerD8) analysis was performed using $CuK\alpha$ radiation ($\lambda = 54056A$). Lattice parameters were calculated by analysis of the X-ray data. The size and particle structure of the prepared powders were studied using TEM (LEO 912AB). Both powder samples were pressed into O ring shapes at pressure of 100 bar, then sintered at 900 °C for 2 h. Scanning electron microscopy (SEM:LEO 1450VP) was used to investigate the surface morphology of the sintered ceramic specimens. Magnetic properties including permeability, AC hysteresis loops, and the Néel temperatures were measured at 77 K at frequencies 10 and 100 kHz. Also, the magnetization of the specimens was measured by VSM technique.

3. Results and discussions

3.1. Characterization

The XRD patterns of the prepared powders calcined at 700 and 800 °C are shown in Figs. 1 and 2, respectively. Fig. 1 indicates that the $CaMnO_{3-\delta}$ structure has not been formed at 700 °C calcination tmperature, but as the patterns in Fig. 2 show the $CaMnO_{3-\delta}$ perovskite with orthorhombic structure (JCPDS 45-1266) has been formed at 800 °C, although a secondary phase ($CaMn_3O_6$) is also observed. The structural parameters and crystallite sizes, estimated from Scherrer formula, are given in Table 1. It is worth nothing that in sol–gel procedure the homogeneity of the cations mixture is of the atomic order which leads to the formation of the final product more easily, whereas in solid-state reaction route we have collection of atoms (particle) and therefore, the formation of the secondary phase is more probable.

Fig. 3(a) shows the TEM image of the $CaMnO_{3-\delta}$ particles synthesized by sol–gel method showing that the particles shape
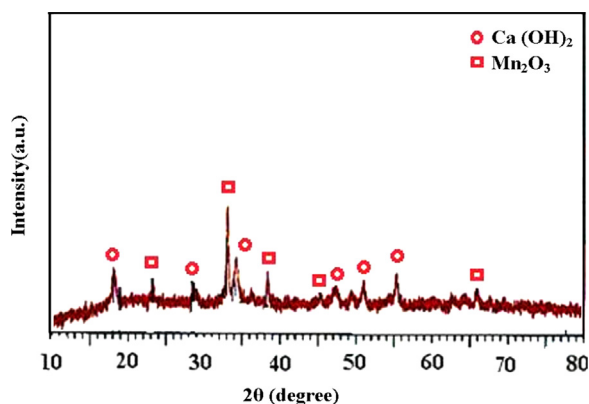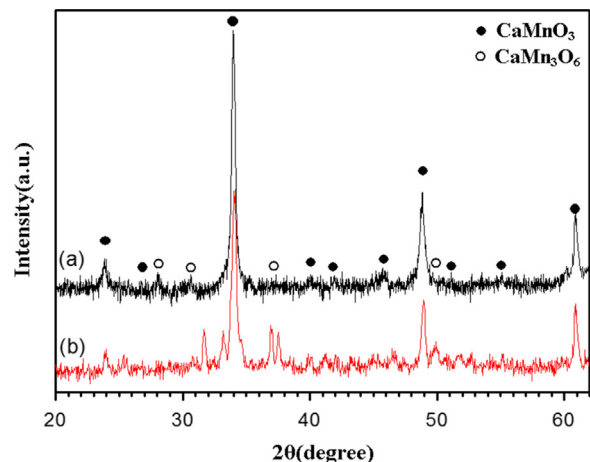

Fig. 2. X-ray powder diffraction patterns of $CaMnO_{3-\delta}$ powders synthesized by (a) sol–gel and (b) solid-state reaction techniques, calcined at 800 °C.

are almost spherical with the average size of 85 nm. TEM image of the particles prepared by solid-state reaction method is given in Fig. 3(b). It can be seen that the particles tend to join to each other and making an agglomerated structure. The SEM image of the $CaMnO_{3-\delta}$ specimens sintered at 900 °C are given in Fig. 4. Fig. 4 (a) shows that the grain size of $CaMnO_{3-\delta}$ ceramic made from the nanopowders prepared by sol–gel method are in the range of 100–200 nm and highly homogeneous in comparison with the grains of the sample made from the nanopowders prepared by solid state reaction, Fig. 4(b).

3.2. Magnetic properties

In order to determine the Néel temperature and to obtain information about the homogeneity of the prepared $CaMnO_{3-\delta}$ ceramics, the magnetic permeability versus temperature were plotted. Permeability was obtained by measuring the inductance of the specimens in coil using an impedance bridge at different temperatures [22]. Samples were cooled in liquid nitrogen and warmed up gradually at a constant rate. The variations of relative magnetic permeability versus temperature at three different frequencies are shown in Fig. 5, which indicates that above $T_{\text{Néel}}$, permeability decreases with increasing temperature. This can be due to disturbing the magnetic domains ordering by increasing the thermal energy more than the energy corresponding to the exchange interaction mechanism, leading to the transition from antiferromagnetic to paramagnetic. The values of the Néel temperature for the two specimens made from powders prepared by both methods, at different frequencies are given in Table 2. In both types of the ceramic specimens, permeability decreases with increasing the frequency and the Néel temperature shifts toward the higher values. This frequency dependence of the magnetic permeability can be explained by displacement of the magnetic walls. In fact, frequency dependence will occur when the magnetic domain walls cannot move fast enough to displace completely before the direction of the magnetic field changes. As the orbital magnetic dipole moments depend on frequency, this temperature dependent of magnetic relaxation is known as spin-lattice correlation [23]. This phenomenon is the ability of the orbital magnetic dipole moment to align with an external magnetic field. Although, the samples prepared by both methods shown almost similar magnetic behavior, the value of the Néel temperature in the ceramic made from sol–gel powders is slightly greater than that of made from solid-state reaction powders. These results can be in relation with the more ferromagnetic component

Fig. 1. X-ray powder diffraction pattern of the prepared powder, calcined at 700 °C.

Table 1
Structural parameters of the prepared $CaMnO_{3-\delta}$ powders.

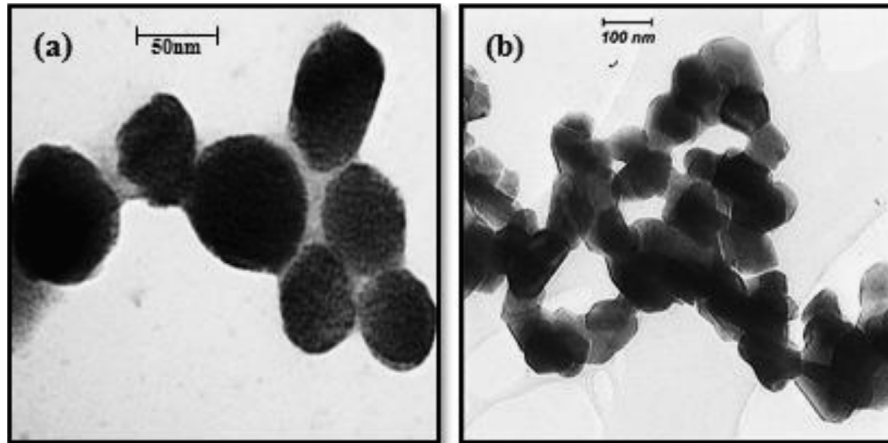| Method	Calcination temperature (°C)	2θ (deg)	d_{hkl} (Å)	(hkl)	Phase	Crystallite size (nm)	Lattice parameter (Å)
Sol–gel	800	34.11	2.62	(220)	Orthorhombic	21/23	$a = 5.282$
		48.87	1.85	(400)		22/72	$b = 7.452$
		60.96	1.52	(422)		20/99	$c = 5.265$
Solid state reaction	800	34.17	2.62	(220)	Orthorhombic	24/75	$a = 5.35$
		49.07	1.85	(400)		30/11	$b = 7.43$
		60.98	1.51	(422)		33/13	$c = 5.28$

Fig. 3. TEM images of $CaMnO_{3-\delta}$ powders calcined at 800 °C prepared by (a) sol–gel and (b) solid-state reaction methods.
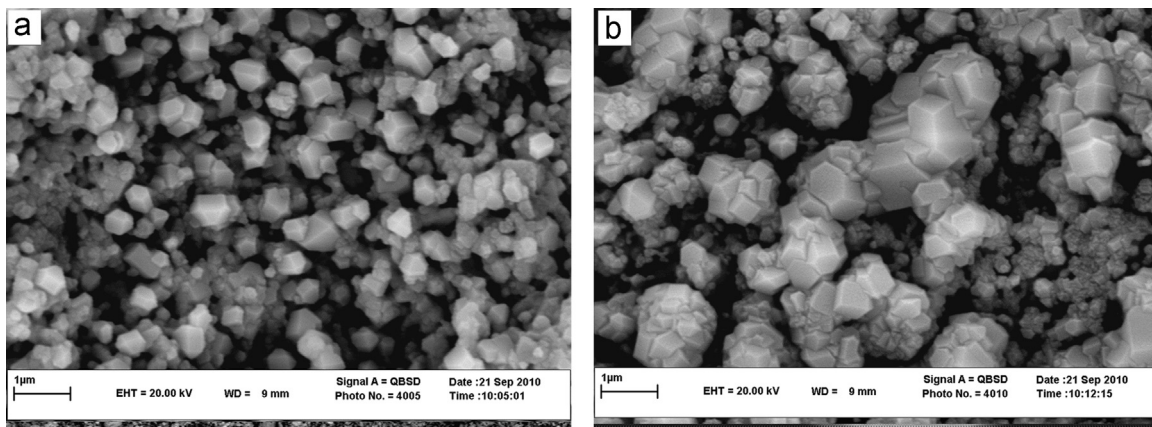

Fig. 4. SEM micrographs of the sintered ceramic specimens made from powders prepared by (a) sol–gel and (b) solid-state reaction routs.
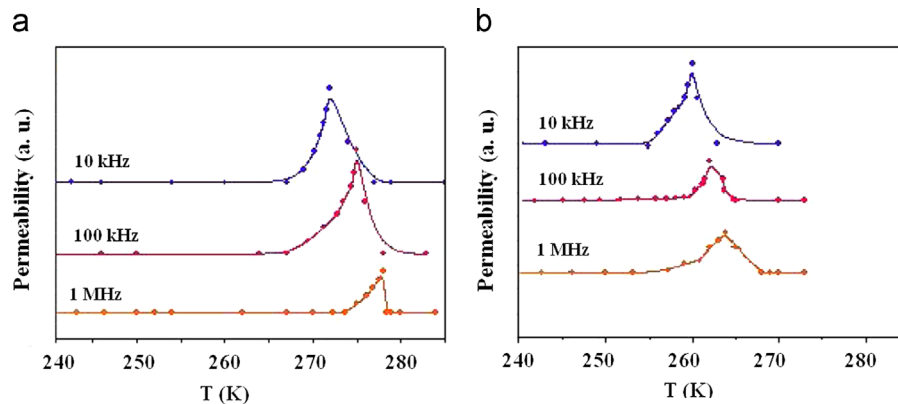

Fig. 5. Magnetic permeability versus temperature for $CaMnO_{3-\delta}$ ceramic specimens made from powders prepared by (a) sol–gel and (b) solid-state reaction at three different frequencies.

as double exchange interaction Mn^{3+}–O–Mn^{4+} in the specimen made from sol–gel powders caused by spin canting at higher temperatures, Fig. 5. In order to study the relaxation behavior and to investigate the presence of ferromagnetic component in both samples, the measured magnetic hysteresis loops below Néel temperature and at room temperature are presented in Figs. 6 and 7, respectively. As shown in Fig. 6, the narrow cycles below the Néel temperature can be related to presence of ferromagnetic components, whereas the linear magnetization depends on the magnetic field corresponding to paramagnetic behavior of both samples at room temperature, Fig. 7. The AC hysteresis measurements were performed

at two different frequencies. The values of coercive and remanence magnetic fields are given in Table 3. As it can be seen, significant increase of coercivity is obtained at higher frequency (100 kHz). In other words, at lower frequency the system has more time to relax to lower energies, leading to lower H_c. With increasing the frequency to higher values, dH/dt increases, and the system has less time to relax, which is known as domain wall pinning [24]. Also, In the case of the ceramic specimen made from sol–gel powder, the coercive field is slightly higher than that of the sample prepared by solid-state reaction. This little difference in

Table 2
Frequency-dependence of the Néel temperature for the prepared $CaMnO_{3-\delta}$ ceramics.

Ceramic specimens made from:	$\nu = 10$ kHz	$\nu = 100$ kHz =	$\nu = 1$ MHz
Sol–gel powders	$T_N = 272$ K	$T_N = 275$ K	$T_N = 277$ K
Solid-state reaction powders	$T_N = 259$ K	$T_N = 262$ K	$T_N = 264$ K

Table 3
Coercive and remnant magnetic fields of $CaMnO_{3-\delta}$ ceramics at $\nu = 10$ and 100 kHz.

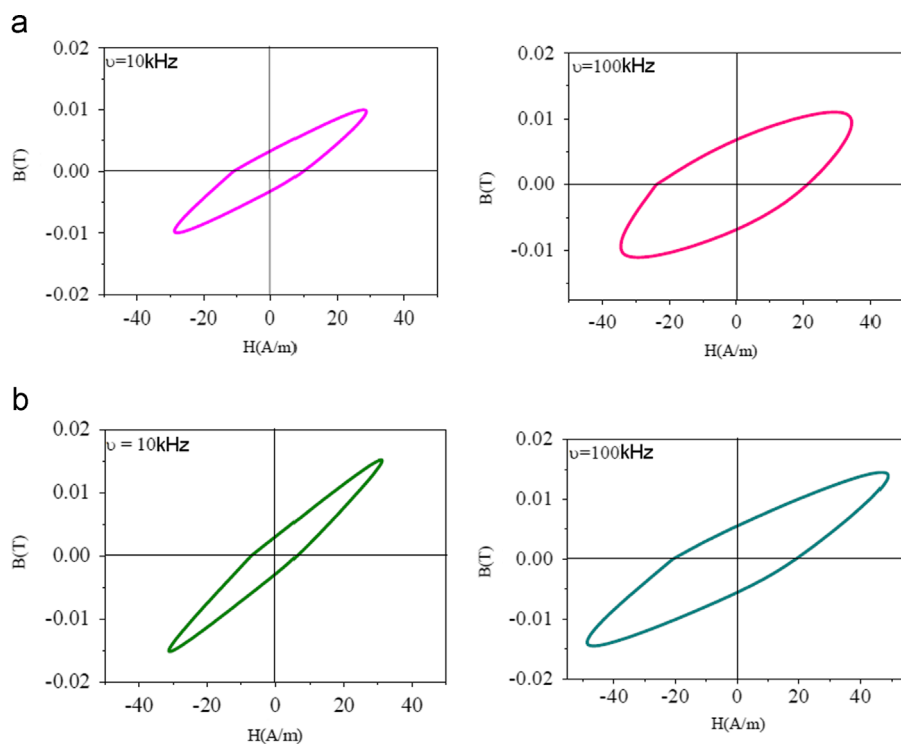| ν (kHz)	Ceramic samples prepared from sol–gel powders		Ceramic samples prepared from solid-state reaction powders	
	H_c (A/m)	B_R (T)	H_c (A/m)	B_R (T)
10	10	0.0034	7	0.003
100	25	0.0078	21	0.006

Fig. 6. AC hysteresis loops of $CaMnO_{3-\delta}$ ceramic specimens made from powders prepared by (a) sol–gel and (b) solid state reaction.
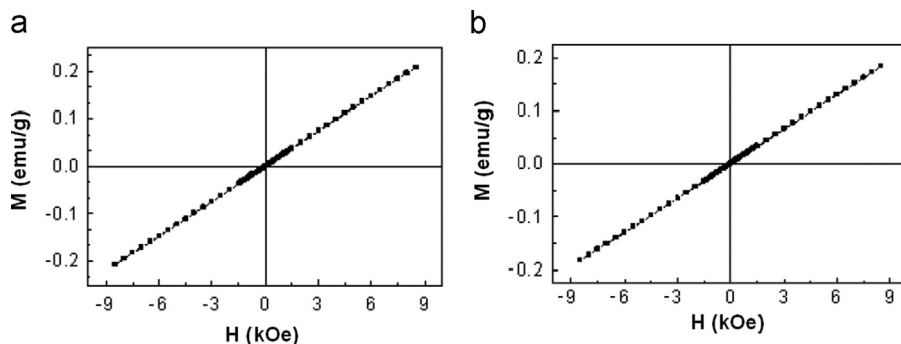

Fig. 7. Magnetization versus applied magnetic field for $CaMnO_{3-\delta}$ ceramics made from powders prepared by (a) sol–gel and (b) solid state reaction, at room temperature.

the coercive field reveals that an anisotropy energy holding the spins along the preferred direction for ceramic specimen made from sol–gel powder is higher due to the more ferromagnetic component (Mn^{3+}–O–Mn^{4+}) as discussed before close to the Néel temperature.

4. Conclusion

$CaMnO_{3-\delta}$ nanopowders were synthesized by sol–gel and solid-state reaction procedures. The X-ray analysis of the powders calcined at 800 °C revealed that both prepared powders have orthorhombic structures. It was found that the formation of orthorhombic phase of $CaMnO_{3-\delta}$, in both procedures, occurs at calcination temperature of 800 °C. TEM images show that the particles prepared by solid- state reaction method tend to join to each other making an agglomerated structure. $CaMnO_{3-\delta}$ ceramic synthesized by sol–gel method has slightly higher phase transition temperature to paramagnetic state and wider hysteresis loop than that of the sample made from powders prepared by solid-state reaction. It was found that the value of the Néel temperature and the shape of hysteresis loops depend on the frequency of the applied magnetic field. Also, the frequency dependence of $T_{Néel}$ and hysteresis loops was found to be the same for both ceramic specimens and can be interpreted by the domain wall pinning phenomenon.

References

[1] D. Flahaut, T. Mihara, R. Funahash, N. Nabeshima, K. Lee, H Ohata, K. Koumoto, Thermoelectrical properties of A-site substituted Ca_{1-x} Re_x MnO_3 system, Journal of Applied Physics 100 (2006) 084911.

[2] W.H. Jung, J.H. Sohn, S.H. Cho, Alternating current electrical properties of $CaMnO_3$ below the Néel temperature, Journal of the American Ceramic Society 83 (2000) 797–930.

[3] A. Souza, J.J. Neumeier, R. Bollinger, B. McGuire, C.A.M. dossantos, K.H. Terashita, Magnetic susceptibility and electrical resistivity of $laMnO_3$, $CaMnO_3$, and $La_{1-x}sr_xMnO_3$ (0.13 ≤ x ≤ 0.45) in the temperature range 300–900 K, Physical Review B: Condensed Matter 76 (2007) 024407.

[4] V. Markovich, E. Rozenberg, Vacancies at Mn-sites in $LaMn_{1-x}O_3$ manganites: interplay between ferromagnetic interactions and hydrostatic pressure, Journal of Applied Physics 95 (2004) 7112.

[5] I. Fita, V. Markovich, G. Gorodetsky, Pressure effect on $Bi_{0.4}Ca_{0.6}Mn_{1-x}Ru_xO_3$ manganite: enhanced ferromagnetism and collapsed exchange bias, Journal of Applied Physics 112 (2012) 093908.

[6] N.N. Loshkareva, Electron-doped manganites based on $CaMnO_3$, Physics of Metals and Metallography 113 (2011) 19–38.

[7] Z. Zeng, M. Greenblatt, Large magnetoresistance in antiferromagnetic $CaMnO_{3-\sigma}$, Physical Review B: Condensed Matter 59 (1999) 8784–8788.

[8] J.M. Porras-Vazquez, T.F. Kemp, P.R. Slater, Synthesis and characterization of oxyanion-doped manganites for potential application as SOFC cathodes, Journal of Materials Chemistry 22 (2012) 8287–8293.

[9] M. Imada, Metal-insulator transitions, Reviews of Modern Physics 70 (1998) 1039.

[10] L.P. Gorkov, V.Z. Kresin, Mixed-valence manganites: fundamentals and main properties, Physics Reports 400 (2004) 149–208.

[11] I. Gil de Muro, M. Insausti, T. Rojo, Morphological and magnetic study of $CaMnO_{3-\sigma}$ oxides obtained from different routes, Solid State Chemistry 178 (2005) 928–936.

[12] E. Bakken, J. Boerio-Goates, T. Grande, B. Hovde, T. Norby, L. Rormark, R. Stevens, S. Stolen, Entropy of oxidation and redox energetics of $CaMnO_{3-\sigma}$, Solid State Ionics 176 (2005) 2261–2267.

[13] J. Hubbard, Electron correlations in narrow energy bands, Proceedings of the Royal Society of London Series A 276 (1963) 238.

[14] P.W. Anderson, H. Hasegawa, Considerations on double exchange, Physical Review 100 (1955) 675–681.

[15] C. Zener, Interaction between the d-shells in transition metals, Physical Review 81 (1951) 440.

[16] J.M.D. Coey, M. Viret, L. Ranno, K. Ounaiela, Electron localization in mixed valence manganites, Physical Review Letters 21 (1995) 3910–3913.

[17] S. Bošković, J. Dukić, B. Matović, Lj. Živković, M. Vlajić, V. Krstić, Nanopowders propertiesand sintering of $CaMnO_3$ solid solutions, Journal of Alloys and Compounds 463 (2008) 282–287.

[18] E.S. Božin, A. Sartbaeva b, H. Zheng, S.A. Wells, J.F. Mitchell, T. Proffen, M.F. Thorpe, S.J.L. Billinge, Structure of $CaMnO_3$ in the range 10 K < T < 550 K from neutron time-of-flight total scattering, Journal of Physics and Chemistry of Solids 69 (2008) 2146–2150.

[19] Q Zhou, B.J. Kennedy, Thermal expansion, and structure of orthorhombic $CaMnO_3$, Journal of Physics and Chemistry of Solids 67 (2006) 1595–1598.

[20] V. Spasojevic, D. Markovic, V. Kusigerski, B. Antic, S. Boskovic, M. Mitric, M. Vlajic, V. Krstic, B. Matovic, Magnetic properties of nano sized mixed valent manganites $CaMnO_3$ and $Ca_{0.7}La_{0.3}Mn_{1-x}Ce_xO_3$ (x=0; 0.2), Journal of Alloys and Compounds 442 (2007) 197–199.

[21] M.E. Melo Jorge, A. Correia dos Santos, M.R. Nunes, Effects of synthesis method on stoichiometry, structure, and electrical conductivity of $CaMnO_{3-\delta}$, International Journal of Inorganic Materials 3 (2001) 915–921.

[22] E. Cedillo, J. Ocampo, V. Rivera, R. Valenzuela, An apparatus for the measuring of initial magnetic permeability as a function of temperature, Journal of Physics E: Scientific Instruments 13 (1980) 383–386.

[23] A.H. Morrish, The Physical Principles of Magnetism, John Wiley & Sons, Inc., New York, 1966.

[24] G. Vertesya, A. Magni, Frequency dependence of coercive properties, Journal of Magnetism and Magnetic Materials 265 (2003) 7–12.